Morphometric analysis of the post-caldera monogenetic volcanoes at Deception Island, Antarctica: implications for landform recognition and volcanic hazard assessment

Dario Pedrazzi (1)*, Gabor Kereszturi (2), Stefania Schamuells (1), Augustin Lobo (1), Janina Calle (3)

(1) ICTJA, CSIC, Group of Volcanology, SIMGEO UB-CSIC, Institute of Earth Sciences Jaume Almera, Lluis Sole i Sabaris s/n, 08028 Barcelona, Spain (*dpedrazzi@ictja.csic.es)
(2) Institute of Agriculture and Environment, Massey University, Palmerston North, New Zealand
(3) Gli Studies & Projects GLISP S.A., Principal Florida Norte s/n, Guayas, Guayaquil, Ecuador

EGU2020-1375

POSVOLDEC (CTM2016-79617-P)
(AEI/FEDER-UE)

1. INTRODUCTION

- Deception Island (DI), South Shetland Archipelago, Antarctica, is an excellent natural laboratory to study monogenetic volcanism as the post-caldera features are recent and well preserved.

- Post-caldera volcanism includes over 30 eruptions during the Holocene, although a considerably higher number of eruptions has been reported (e.g. *Orheim, 1971*).

- Recent eruptions in 1967, 1969 and 1970 (*Baker et al., 1975*; *Smellie, 2002*; *Pedrazzi et al., 2014*; *2018*) have shown that volcanic activity on DI can become a concern for tourists, scientists and military personnel working on or near the island and it is not possible to rule out the possibility of a future eruption.

Southern view of Deception Island caldera. Picture taken from Mount Pond. Credits Dario Pedrazzi (2013).

- Volcanic hazard assessment requires information to be obtained from the geomorphology of volcanic edifices and deposits characteristics, such as volumes, crater shapes, grain size distributions, and edifice geometries.

- The objective of this work is to identify the eruptive processes and evolution of post-caldera monogenetic volcanic edifices at DI by morphometric analysis, supported by field observations from three field campaigns in 2011, 2013 and 2018.

- Morphometric analysis of monogenetic volcanoes formed from magma-water interactions is often lacking, compared to scoria cones, hence this study aims to contribute by analysing the morphology of young tuff rings and tuff cones from DI.

- Since, DI post-caldera volcanism is mainly <4,000 years old (*Antoniades et al., 2018*), it provides an opportunity to incorporate geomorphological observations to comprehend better the potential evolution of a future eruption for a broader understanding of volcanic hazards.

2. GEOLOGICAL SETTING AND GENERAL CHARACTERISTICS OF DECEPTION ISLAND

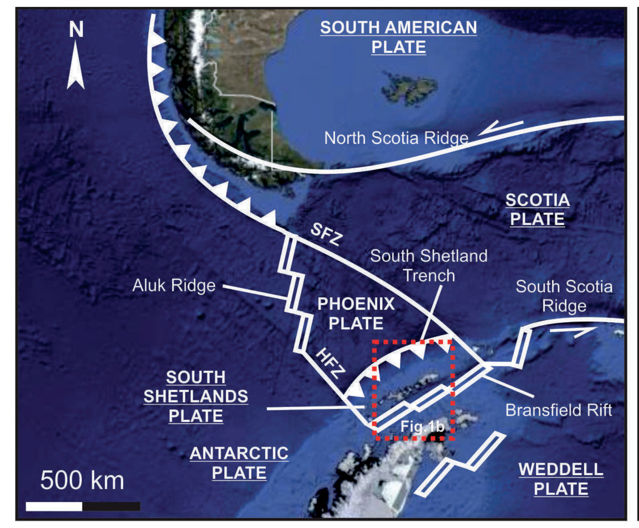

Simplified regional tectonic map and location of the South Shetland Islands Archipelago (modified from Ibañez et al., 2003). HFZ-Hero Fracture Zone, SFZ-Shetland Fracture Zone.

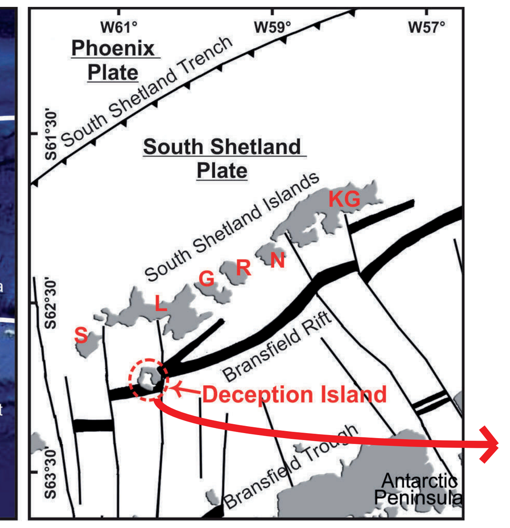

S-Snow Island, L-Livingston Island, G- Greenwich Island, R-Robert Island, N-Nelson Island, KG-King George Island.

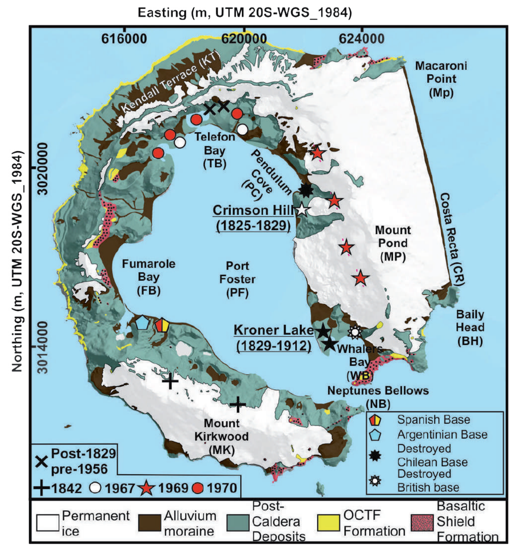

Simplified geological map of Deception Island (after Smellie et al., 2002; Martí et al., 2013).

- DI is located at the south-western end of the Bransfield Strait.

- DI consists of a horseshoe-shaped volcanic edifice (< 0.75 Ma; *Valencio et al., 1979*; Smellie, 1988).

- Three main phases lead to the formation of DI: pre-, syn- and post-caldera (*Smellie et al., 2002*; *Martí et al., 2013*).

- Historical post-caldera volcanism (1829 – 1970) on DI is characterised by monogenetic small-volume basaltic eruptions (< 0.1 km^3) of VEI 2 or 3 magnitude events.

- Recent explosive eruptions were driven by magma-water interaction, as the last eruptive episodes that took place between 1967 and 1970 (*Baker et al., 1975*; *Roobol, 1982*; *Smellie, 2001*; *Pedrazzi et al., 2014; 2018*).

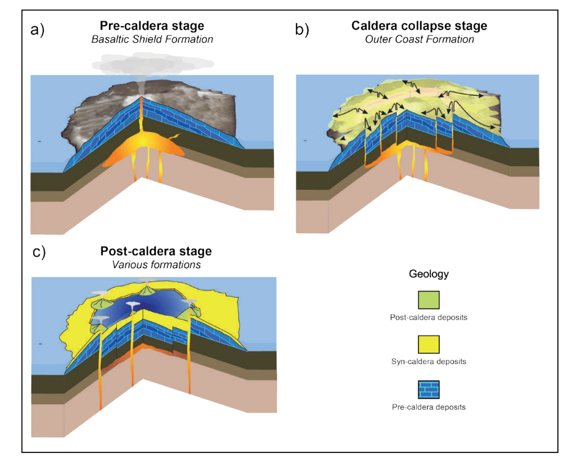

Simplified sketch illustrating the formation of the Deception Island caldera (after Martí et al., 2013).

3. METHODS

- Antarctic campaigns: RECALDEC in 2010-2011, PEVOLDEC in 2012-2013 and POSVOLDEC in 2017-2018;

- The source data used for the spatial localization, morphology and morphometric analysis of DI cones are:
i. the modified geological map of *Martí et al. (2013)*;
ii. the geomorphological map of the island at 1:25.000 (*López-Martínez et al., 2002*);
iii. the Digital Elevation Model (DEM), accuracy in a 2m x 2m raster.

- The morphometric parameters used in this study are (*Wood, 1980a, b*):
i. crater maximum (Cmax) and minimum (Cmin) diameter;
ii crater width (Ccrater);
iii crater depth (Dcr);
iv. cone maximum (Wmax) and minimum (Wmin) diameter;
v. cone width ratio (Wco);
vi. cone height (Hcomax and Hcomin);
vii. mean cone height (Hco).

- DEM-based slope angle calculations were performed to obtain:
i. cone slope parameters: Smax, Smin, Smean, Smedian;
ii. crater slope parameters: Scrmax, Scrmin, Scrmean, Scrmedian.

- The morphometric analysis was performed through the Quantum GIS, version Bonn (https://www.qgis.org/en/site/) and R-Studio software (https://www.rstudio.com/).

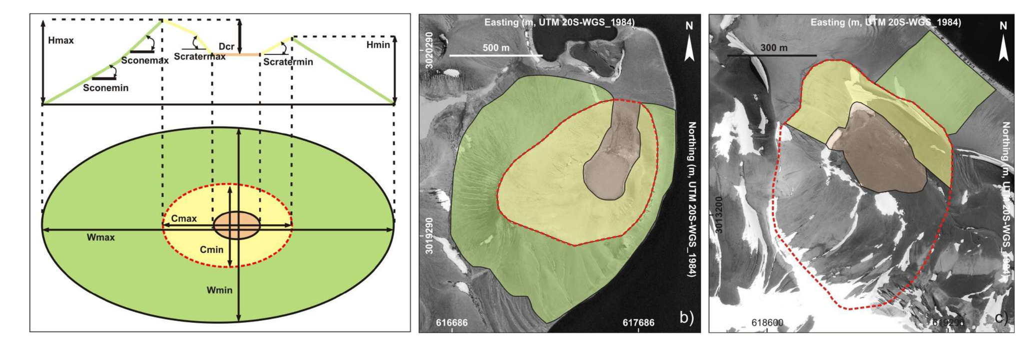

Morphometric parameters of DI's craters and cones.

5. DISCUSSION AND CONCLUSIONS

- At DI, more than 100 volcanic structures (including volcanic cones and/or craters) were observed.

- This study suggests that most of the monogenetic volcanoes, formed after the caldera collapse on Deception Island, show low geomorphic profiles (Hco/Wco values from 0.01 to 0.16) and associated median slope angles that are typically lower than 25°, except for a few cones.

- These characteristics, as well as the physical properties of the exposed outcrops (poorly vesiculated bombs and lapilli scoria deposits, high lithic content, and palagonitisation of glass in the matrix), are mostly consistent with a hydrovolcanic origin.

- Overlapping craters and cone have been developed almost throughout the island being mostly in areas of greater topography.

- The histograms of slope angles of the volcanic structures at DI are complex since they present a multimodal and skewed distribution.

- In the same way, polar diagrams show variabilities among the different volcanic landforms.

- The morphometric analysis helped to discriminate between tuff cones and tuff rings. However, there is a gradual continuum of geometries in-between those end-member landforms.

- The described geometries and morphologies are interpreted to be rather formed during the eruptive processes with a secondary imprint from erosional activity.

- This study shows that the geomorphological approach developed for "dry" scoria cones and DEM-based methodologies can be applied to "wet" hydrovolcanic volcanoes, such as tuff rings and tuff cones.

- At DI, most of the craters were well preserved, allowing morphometric parameters to be obtained while the same type of analysis was only possible for some cones due the frequent overlapping and erosion.

- Hydrovolcanic activity forming tuff rings/maars and tuff cones, is considered the major cause of volcanic hazards at DI.

- Hazard implications of the eruption styles have shifted from the early Surtsey-type to phreatomagmatic due to spatial changes in the availability of the external water within an actively evolving collapse caldera basin. This aspect of the evolution of DI needs to be investigated in the future.

4. TUFF CONES VS TUFF RINGS

TUFF CONES

CROSS HILL

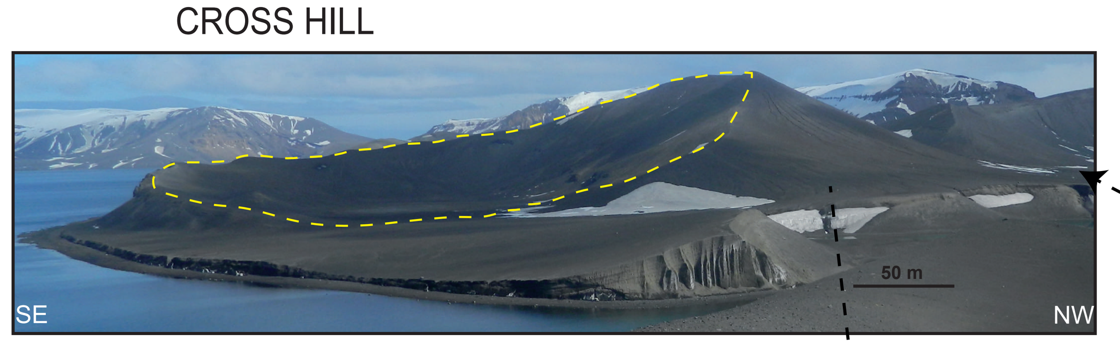

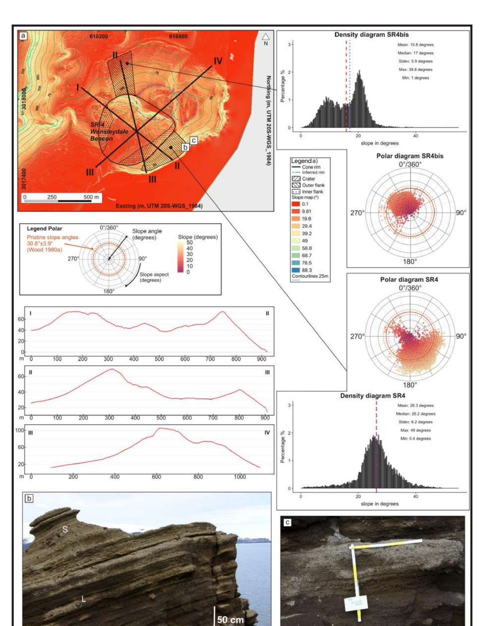

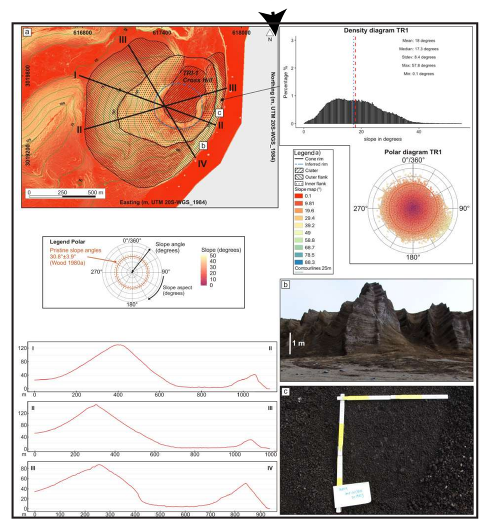

WENSLEYDALE BACON

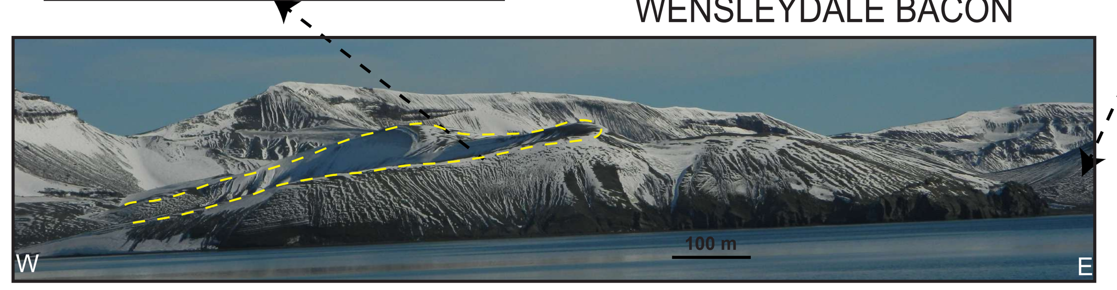

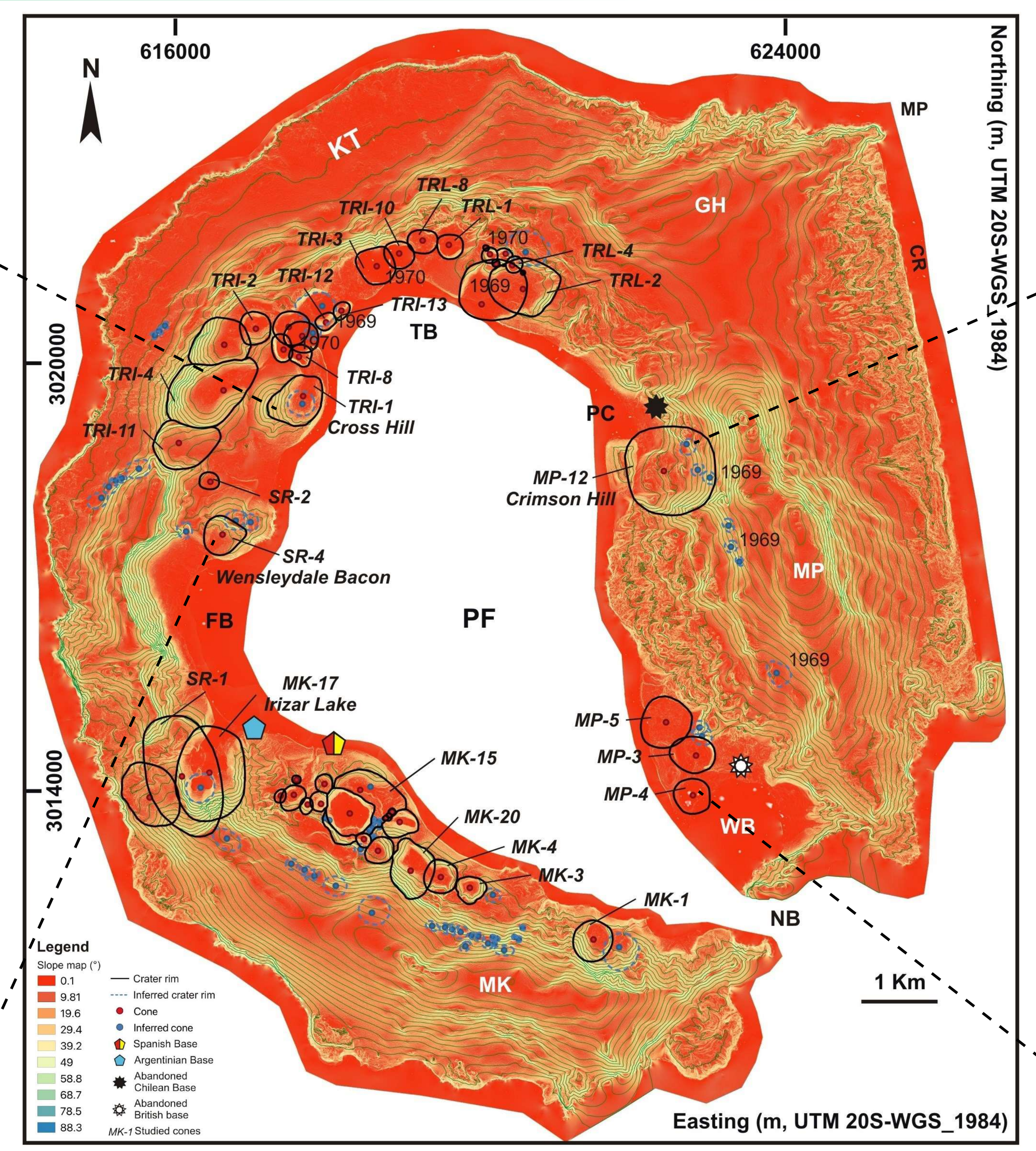

Slope map of Deception Island with the location of the post-caldera explosive vents (red-well-preserved and blue-inferred dots). CR-Costa Recta, FB-Foster Bay, GH-Goddard Hill, KT-Kendall Terrace, MK-Mount Kirkwood, MP-Mount Pond, MPO-Macaroni Point, NB-Neptune Bellows, PC-Pendulum Cove, PF-Port Foster, TB-Telefon Bay, WB-Whalers Bay.

TUFF RINGS

CRIMSON HILL

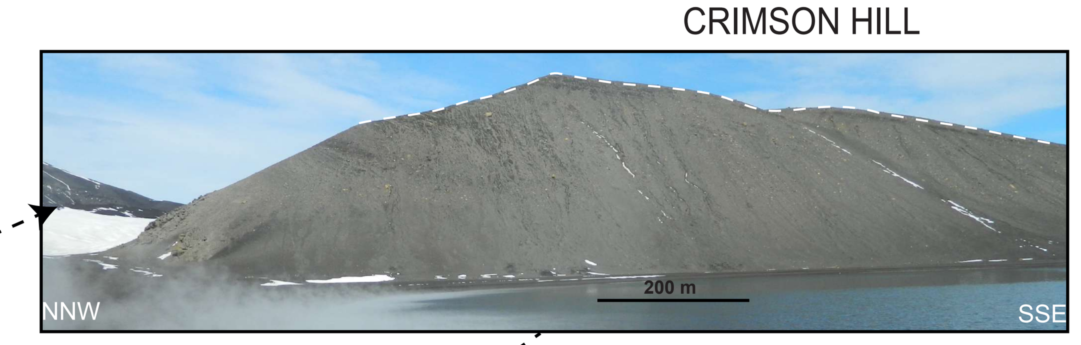

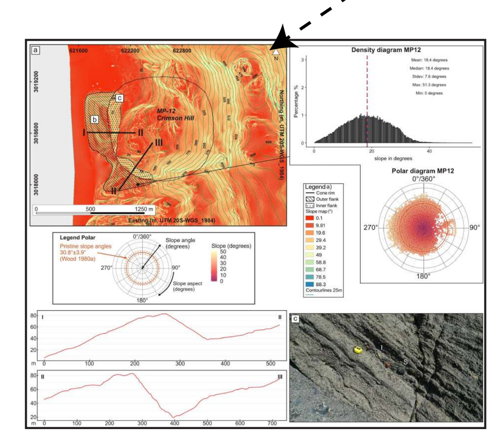

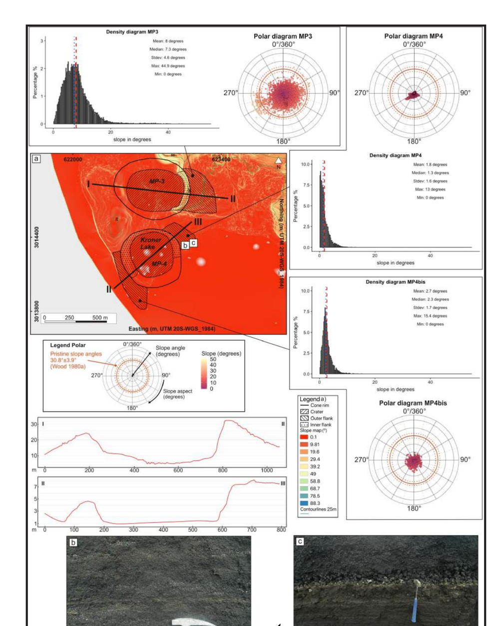

KRONER LAKE

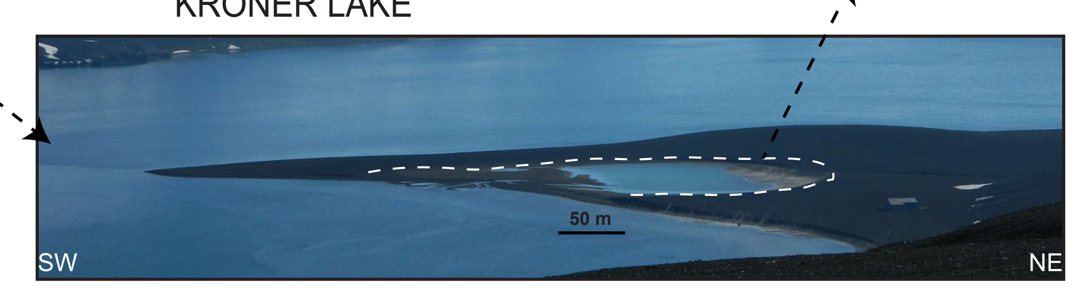

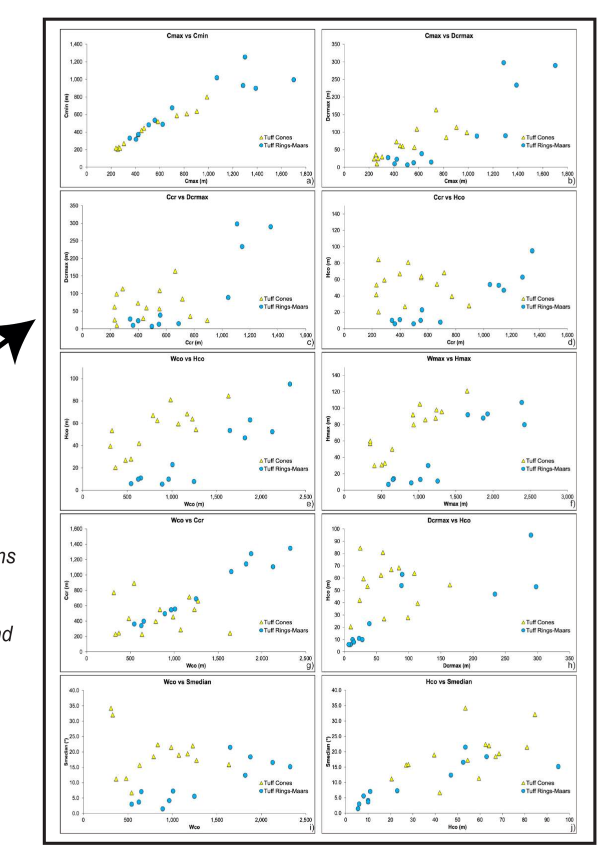

Morphometric relations for DI craters and cones, highlighting fields of tuff cones and rings.

- Morphometric parameters allowed to discriminate between two types of landforms: tuff cones and tuff rings.

- Tuff cones are located in general in the western and northern side of DI: Mount Kirkwood, Fumarole and Telefon Bay;

- Typically, they are made of clast-supported deposits, sometimes yellow to brown coloured and characterised by lithic-rich tephra and (in some cases laminated) thinly to thickly bedded lapilli and ash beds with bombs. The deposits are occasionally palagonitised;

- Tuff rings were mainly identified in the eastern part of DI: Mount Pond;

- The deposits mainly consist of thinly to thickly bedded (in some cases palagonitised) lapilli and ash deposits with dunes and cross-bedding.

REFERENCES

- **Antoniades D., Giralt S., Geyer A., Álvarez-Valero A.M., Pla-Rabes S., Granados I., Liu E.J., Toro M., Smellie J.L., Oliva, M. (2018).** The timing and widespread effects of the largest Holocene volcanic eruption in Antarctica. Scientific reports, 8(1): 17279.
-**Baker P.E., McReath I., Harvey M.R., Roobol M.J., Davies T.G. (1975).** The geology of the South Shetland Islands. V. Volcanic evolution of Deception Island. British Antarctic Survey. 78:81 PP.
-**Ibáñez J.M., Almendros J., Carmona E., Martí C., Abril, M. (2003).** The recent seismo-volcanic activity at Deception Island volcano. Deep-Sea Res II Top Stud Oceanogr 50(10):1611–1629.
-**López-Martínez J., Serrano, E. (2002).** Geomorphology. In: López-Martínez, J., Smellie,J.L., Thomson, J.W. & Thomson, M.R.A. (eds) Geology and Geomorphology of Deception Island. British Antarctic Survey, Cambridge, BAS GEOMAP Series, Sheets 6-A and 6-B, 1:25 000, 31-39.
-**Martí .J, Geyer A., Aguirre-Diaz G. (2013).** Origin and evolution of the Deception Island caldera (South Shetland Islands, Antarctica). Bull Volcanol 75(6):732.
-**Orheim O. (1971).** Volcanic activity on Deception Island, South Shetland Islands. In: ADIE RJ (ed) Antarctic geology and geophysics. Universitetsforlaget, Oslo, pp 117–120.
-**Pedrazzi D., Aguirre-Díaz G., Bartolini S., Martí J., Geyer A. (2014).** The 1970 eruption on Deception Island (Antarctica): eruptive dynamics and implications for volcanic hazards. J Geol Soc 171(6):765–778.
-**Pedrazzi D., Németh K., Geyer A., Álvarez-Valero A. M., Aguirre-Díaz G., Bartolini, S. (2018).** Historic hydrovolcanism at Deception Island (Antarctica): implications for eruption hazards. Bulletin of Volcanology 80(1): 11.
-**Roobol M.J. (1982).** The volcanic hazard at Deception Island, South Shetland Islands. Brit Antarc Surv Bull 51:237-245.
-**Smellie JL (1988)**. Recent observations on the volcanic history of Deception Island, South Shetland Islands. Brit Antarct Surv Bull 81:83.
-**Smellie J.L. (2001).** Lithostratigraphy and volcanic evolution of Deception Island, South Shetland Islands. Antarct Sci 73(2):788–209.
-**Smellie J.L. (2002).** The 1969 subglacial eruption on Deception Island (Antarctica): events and processes during an eruption beneath a thin glacier and implications for volcanic hazards. Geol Soc Lond, Spec Publ 202(1):59–79.
-**Smellie J.L., López-Martínez J., Headland R.K., Hernández-Cifuentes F., Maestro A., Millar I.L., Rey J., Serrano E., Somoza L., Thomson J.W. (2002).** Geology and geomorphology of Deception Island. (BAS Geomap Series, Sheets 6A and 6B) 77pp.
-**Valencio D.A., Mendía J., Vilas J.F. (1979).** Palaeomagnetism and KAr age of Mesozoic and Cenozoic igneous rocks from Antarctica. Earth Planet Sci Lett 45(1):61–68.
-**Wood C.A. (1980a).** Morphometric analysis of cinder cone degradation. J Volcanol Geotherm Res 8(2–4):137–160.
-**Wood, C.A. (1980b).** Morphometric evolution of cinder cones. J. Volcanol. Geotherm. Res., 7(3-4): 387-413.

FOR MORE INFORMATION

POSVOLDEC | ABOUT ME | ICTJA-CSIC

This research was supported by the MICINN grant CTM2011-13578-E and was partially funded by the POSVOLDEC project (CTM2016-79617-P) (AEI/FEDER-UE). A.G. is grateful for her Ramón y Cajal contract (RYC-2012-11024). D.P. is grateful for his Beatriu de Pinós (2016 BP 00086) and Juan de la Cierva (IJCI-2016-30482) contracts. This research is part of POLARCSIC and AntVolc activities.